# Fundamentals of fuel cell system integration*

Michael Krumpelt**, Romesh Kumar and Kevin M. Myles

*Argonne National Laboratory, Chemical Technology Division, 9700 South Cass Avenue, Argonne, IL 60439 (USA)*

## Abstract

Fuel cells are theoretically very efficient energy conversion devices that have the potential of becoming a commercial product for numerous uses in the civilian economy. We have analyzed several fuel cell system designs with regard to thermal and chemical integration of the fuel cell stack into the rest of the system. Thermal integration permits the use of the stack waste heat for the endothermic steps of fuel reforming. Chemical integration provides the steam needed for fuel reforming from the water produced by the electrochemical cell reaction. High-temperature fuel cells, such as the molten carbonate and the solid oxide fuel cells, permit this system integration in a relatively simple manner. Lower temperature fuel cells, such as the polymer electrolyte and phosphoric acid systems, require added system complexity to achieve such integration. The system economics are affected by capital and fuel costs and technical parameters, such as electrochemical fuel utilization, current density, and system complexity. At today's low fuel prices and the high fuel cell costs (in part, because of the low rates of production of the early prototypes), fuel cell systems are not cost competitive with conventional power generation. With the manufacture and sale of larger numbers of fuel cell systems, the total costs will decrease from the current several thousand dollars per kW, to perhaps less than US$ 100 per kW as production volumes approach a million units per year.

## Introduction

Fuel cells are at the crossroads of either continuing to be a reliable but expensive power source for space and military applications or becoming a commercial product for numerous uses in the civilian economy. Compared with combustion-based heat engines, fuel cells have very low emissions and noise, and are potentially more efficient. If capital costs were equivalent, fuel cells could replace turbines and reciprocating combustion engines in stationary and mobile applications. However, fuel cells are not yet produced in large enough quantities to be cost competitive with established technology in a broad range of applications; the lower operating costs are not sufficient to compensate for the still fairly high capital costs. Commercialization is thus challenging for the developers. Nevertheless, as more and more unique applications are found, production volumes will increase, and costs will come down. Eventually, fuel cells may

---

*The submitted manuscript has been authored by a contractor of the US Government under contract No. W-31-109-ENG-38. Accordingly, the US Government retains a nonexclusive, royalty-free license to publish or reproduce the published form of this contribution, or allow others to do so, for US Government purposes.
**Author to whom correspondence should be addressed.

be widely used as dispersed power generators, in cogeneration systems, in utility grids, and in electric vehicles for transportation.

In this article, the fundamental issues in system design and integration are discussed for the five major types of fuel cells. Efficiencies of individual stacks and complete systems are defined; thermal management and internal fuel reforming are discussed; the trade-offs between system efficiency and cost, as well as cost versus production volume, are explored.


**Efficiency**

Fuel cells are more efficient energy conversion devices than heat engines because the chemical energy of the fuel is converted directly to electricity instead of first being transformed to heat, then mechanical energy, and finally to electricity. In theory, the energy conversion efficiency of a fuel cell, $\epsilon_{fc}$, is given by the ratio of the free energy of the cell reaction at the cell's operating temperature, $\Delta G_T$, to the enthalpy of reaction at standard state, $\Delta H^0$:

$$\epsilon_{fc} = \frac{\Delta G_T}{\Delta H^0} \tag{1}$$

A hydrogen/oxygen fuel cell operating at 100 °C has a theoretical efficiency of 83% based on the higher heating value (HHV) of hydrogen, or 91% based on the lower heating value (LHV). In either case, the standard state temperature is 25 °C but the product water is in the liquid state for the HHV and in the gas state for the LHV. In this paper we use the HHV as the basis for efficiencies.

Not even the best of the heat engines can come close to such high theoretical conversion efficiencies since none can operate at the flame temperature of hydrogen. As pointed out by Appleby and Foulkes [1], materials limitations are the reason for the lower efficiency of heat engines, and not the Carnot principle as such.

In practice, as always, efficiencies considerably lower than the theoretical values have to be accepted. Implicit in the definition of the theoretical efficiency is that the fuel cell operates at the equilibrium potential given by the Nernst equation:

$$E^0 = \frac{-\Delta G_T}{nF} \tag{2}$$

where $E^0$ is the equilibrium potential, $n$ the number of electrons transferred in the cell reaction and $F$ the Faraday constant. The operating potential, $E$, of the fuel cell depends on the current density:

$$E = E^0 - (a_{an} + a_{ca}) - (b_{an} + b_{ca}) \frac{RT}{nF} \ln i - Ai \tag{3}$$

where $a$ and $b$ are characteristic constants for the electrochemical reactions at each electrode, the subscripts 'an' and 'ca' refer to the anode and the cathode, respectively, $R$ is the gas constant, $T$ the cell temperature, $A$ the area-specific resistance of the fuel cell, and $i$ is the current density in the cell.

Further, when the fuel and oxidant are not just pure reactants but contain inert gases as well, two other adjustments need to be made to the fuel cell's operating potential. First, the electrochemical utilization of the fuel cannot be 100% because the electrode reactions then become diffusion limited. For fuel gas mixtures containing

hydrogen, the operating fuel utilization, $U_f$, is often specified to be 70 to 85%, requiring a corresponding reduction of the fuel cell efficiency (but not necessarily a matching reduction in the system efficiency). Second, because the reactants in the fuel and oxidant gases are gradually depleted as the gases flow from the inlet to the exit of the fuel cell, the 'local' Nernst potential varies across the cell. In a cell operating at 85% fuel utilization and 50% oxygen utilization, the minimum Nernst potential may be as much as 100 mV lower than the maximum.

Computer codes are usually used to calculate the Nernst potential and other parameters for a fuel cell operating under given conditions. Such codes typically iterate the local variations in fuel and oxidant gas compositions, cell temperatures, materials resistivities and other properties, and heat- and mass-transfer effects across a nodal network of the fuel cell area. For example, Fig. 1 shows the variations in the calculated Nernst potential, current density, and temperature for a cross-flow molten carbonate fuel cell of 1 m² area.

A less rigorous approximation of the effective Nernst potential can be obtained by 'averaging' the fuel and oxidant concentrations from the inlet to the outlet:

$$E_N = E^0 - \frac{RT}{nF} \log \text{ mean } c_f - \frac{RT}{nF} \log \text{ mean } c_{ox} \tag{4}$$

where $c_f$ and $c_{ox}$ refer to the concentrations of the fuel and the oxidant, respectively. Then the overall efficiency of the fuel cell may be approximated by:

$$\epsilon_{fc} = \frac{nF[E^0 - \sum a - \sum b \frac{RT}{nF} \ln i - Ai - \frac{RT}{nF} (\log \text{ mean } c_f + \log \text{ mean } c_{ox})]}{\Delta H^0} U_f \tag{5}$$

In most applications, the system will contain blowers, pumps and other power-consuming components but may also include bottoming cycles that generate additional power. Thus, the net system efficiency, $\epsilon_{system}$, can vary, depending on the complexity of the system and on the operating voltage of the fuel cell; it is best defined by the ratio of net electrical power generated to the heating value of the fuel:

$$\epsilon_{system} = \frac{\text{net electrical power}}{\Delta H^0} \tag{6}$$

Thus, in some of today's admittedly non-optimized systems, the net efficiencies may be only about 40%.

## Types of fuel cells

Fuel cells were first used effectively in space applications where pure hydrogen and oxygen are available. In terrestrial systems, the hydrogen has to be generated from hydrocarbon, fossil, or biomass sources, yielding a gas mixture that contains hydrogen, carbon dioxide, carbon monoxide, water, and perhaps nitrogen. The alkaline fuel cell (AFC) currently used in the US space shuttle cannot tolerate carbon dioxide. The polymer electrolyte fuel cell (PEFC), also originally developed for space applications and used in the Gemini program, is highly sensitive to carbon monoxide. To accommodate hydrocarbon fuels for terrestrial applications, therefore, the phosphoric acid fuel cell (PAFC), the molten carbonate fuel cell (MCFC), and the solid oxide fuel cell (SOFC) were developed. Operating at progressively higher temperatures (200 to 1000 °C),
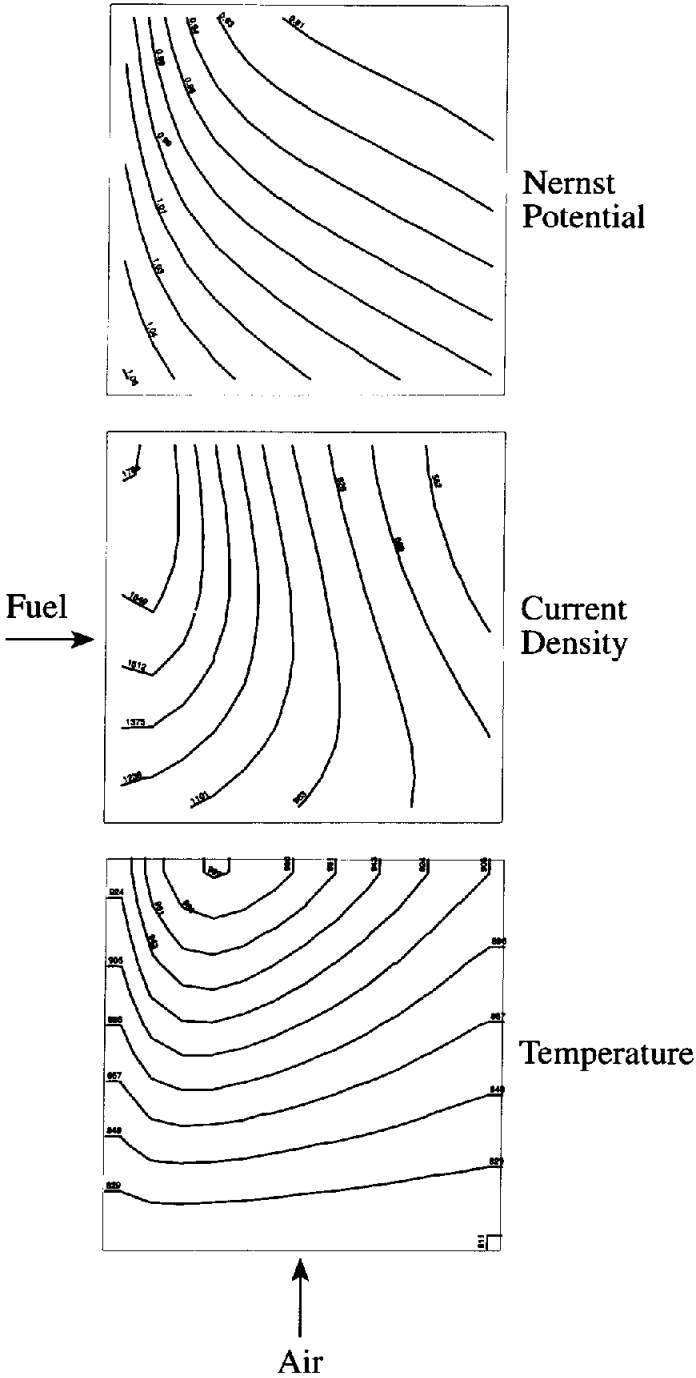
Fig. 1. Calculated Nernst potential, current density, and temperature profiles for 1 m×1 m cross-flow molten carbonate fuel cell with 85% fuel utilization and 50% oxidant utilization.

these fuels cells cannot only tolerate the oxides of carbon, but the MCFC and the SOFC can actually use carbon monoxide (or even methane) directly as the fuel.

The higher the operating temperature of the fuel cell, the simpler the fuel processing becomes, as will be illustrated below. The cell's operating temperature also has a major impact on the thermodynamics and kinetics of the fuel cell processes, as shown in Table 1. The equilibrium potential $E^0$ can be as high as 1.16 V in low-temperature cells, decreasing to 0.925 V at 1000 °C. The overpotential losses at the anode and the cathode, however, also decrease with rising temperatures [2] since reaction kinetics are generally improved. The two effects off-set each other at the lowest and the highest temperatures, but in the temperature range between 400 and 700 °C, the thermodynamic and kinetic conditions are optimal for fuel cell operation.

The conductivities of the electrolytes are actually very similar in all five types of fuel cell [1, 3–5], suggesting that resistive losses should be of roughly the same order of magnitude for each cell type. In reality, the tubular SOFC has rather high resistive losses due to the long current path; on the other hand, the PEFC has low resistive losses, because the membranes used are thin. Regardless of the operating temperature, the actual fuel cell operating voltages are typically between 0.7 and 0.8 V in pressurized systems [1, 6, 7], and between 0.6 and 0.7 V in atmospheric pressure systems [7]. These cell voltages correspond to fuel cell efficiencies of 40 to 55%; complete system efficiencies are somewhat lower.

In any of these types of cells, generally about half of the energy content of the fuel is released as heat, which must be removed from the fuel cell stack. This heat may either be used somewhere else in the system or rejected to the environment. In the next section, we discuss some thermal integration options, using the PAFC as an example. Following that, integration of fuel processing with the fuel cell is described for the SOFC.

## System integration

### Thermal integration

Figures 2 and 3 illustrate the thermal system integration for two designs of PAFC systems: one by ONSI Corporation and the other by Argonne. Figure 2 shows the flow diagram for the 200-kW commercially available power plant offered by ONSI [8]. Natural gas at ambient pressure passes through a desulfurizer and is then mixed with steam before entering the reforming reactor, where it is converted to hydrogen and carbon monoxide over a nickel catalyst:

$$CH_4 + H_2O \longrightarrow 3H_2 + CO \qquad \Delta H_{298} = +206.2 \text{ kJ} \tag{7}$$

The reformate is cooled and then passed over a low-temperature shift catalyst to convert most of the CO to $CO_2$:

$$CO + H_2O \longrightarrow H_2 + CO_2 \qquad \Delta H_{298} = -41.2 \text{ kJ} \tag{8}$$
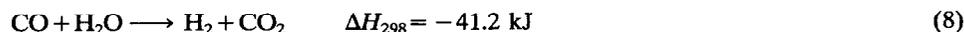
because PAFCs can tolerate only about 0.5% CO without a significant degradation in performance. Most of the hydrogen-rich gas is electrochemically oxidized in the fuel cell, and the rest is combusted in the burner that supplies heat for the endothermic reforming reaction.

Even this simple system has some chemical and thermal integration of the fuel cell stack with the fuel processor by providing steam and residual fuel to the reforming reactor. Excess heat is removed from the fuel cell stack by evaporative cooling with

TABLE 1

Characteristics of the different types of fuel cells

| Fuel cell | Electrolyte | Operating temperature (°C) | Equilibrium potential (V) | Overpotentials (V) | Conductivity of electrolyte ($\Omega^{-1}$ cm$^{-1}$) | Stack operating potentials (V) | |
|---|---|---|---|---|---|---|---|
| | | | | | | 1 atm | pressurized |
| PEFC | $-(CF_2)_m-SO_3H$ | 80 | 1.160 | 0.28 [2] | 0.1–0.2 [3] | | 0.75 [6] |
| AFC | KOH | 100 | 1.150 | 0.22 [2] | 0.17 [1] | | 0.86 [1] |
| PAFC | $H_3PO_4$ | 200 | 1.130 | 0.30 [2] | 0.15 [1] | 0.65 [7] | 0.71 [7] |
| MCFC | $Li_2CO_3-K_2CO_3$ | 650 | 1.020 | 0.06 [2] | 0.14 [4] | 0.66 [7] | 0.75 [7] |
| SOFC | $Zr_{0.92}Y_{0.08}O_{2.96}$ | 1000 | 0.925 | 0.05 [2] | 0.12 [5] | 0.60 [7] | |
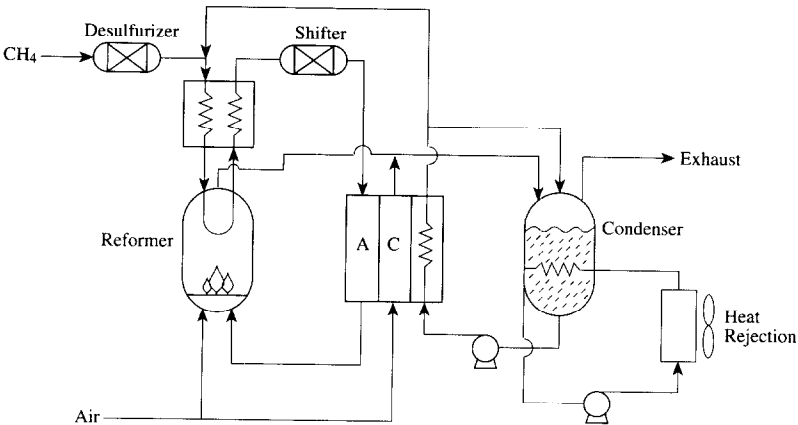
Fig. 2. Schematic diagram of the 200-kW phosphoric acid fuel cell system developed by ONSI. System operates at atmospheric pressure with natural gas fuel.
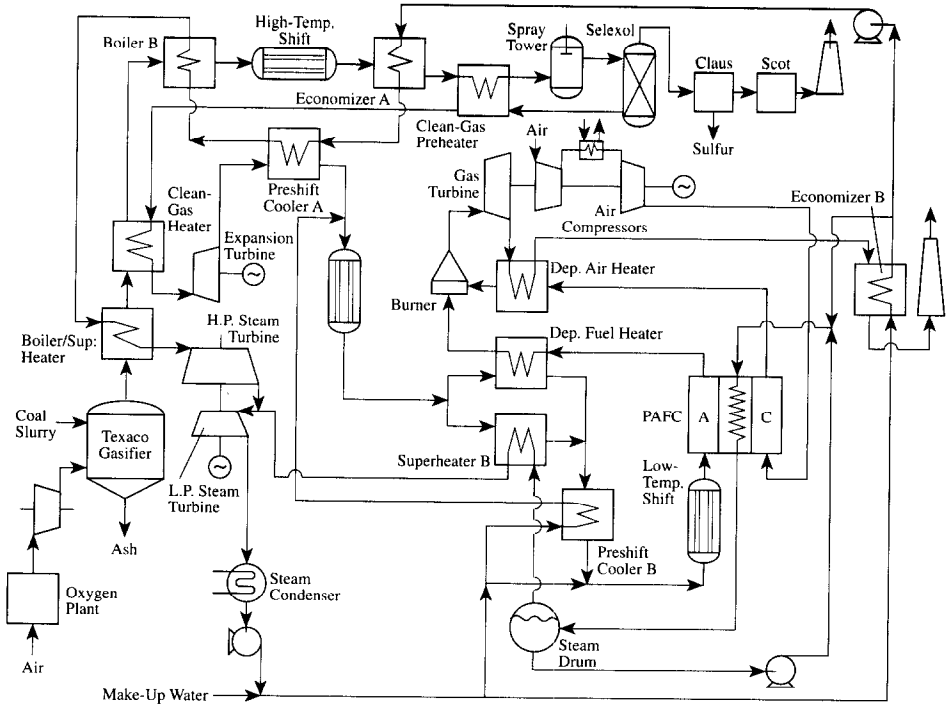


Fig. 3. System design for a phosphoric acid fuel cell system developed by Argonne for a base-load utility central station plant. System operates under pressurized conditions with coal gas fuel.

water. A part of the steam that is produced is used for reforming the natural gas; the rest goes to the water recovery unit, where a secondary water cooling loop removes the heat from the system. This system has an electrical efficiency of 36% and very

low levels of pollutant emissions (0.8 ppm $NO_x$, 3.6 ppm CO, 0.006 ppm $SO_x$, 0.6 ppm non-methane hydrocarbons).

An example of a much more integrated, but also more complex, system design for the same type of fuel cell is shown in Fig. 3. This base-load plant design is for a utility central station operating on coal and was developed and analyzed at Argonne [9]. Coal is converted to syngas in a pressurized entrained-bed gasifier. The hot syngas is cooled in a superheater generating steam for a high pressure turbine. Some of the carbon monoxide is converted to hydrogen in the high-temperature shift reactor, before the syngas is desulfurized by solvent extraction. The clean syngas is reheated and then expanded to the 10 atm operating pressure of the fuel cell. Following the expansion turbine are intermediate- and low-temperature shift reactors. The hydrogen-rich fuel is electrochemically oxidized, and the depleted fuel leaving the fuel cells is combusted in a gas turbine. As in the atmospheric-pressure PAFC system, heat is removed from the fuel cells by evaporative cooling with water; the product steam is used to drive the low-pressure side of the steam turbine.

Modeling of this system yields a system efficiency of 42.40%, with 55% of the total electric power coming from the fuel cells, 21% from the gas turbine and 24% from the steam turbine. A complete accounting of the energy flow in this system is shown in Fig. 4. The reader may note that the gross efficiency is 47.55%, but 3.28% of the input energy is needed for air compression in the oxygen plant, 1.69% of the input energy is consumed by various electric motors and 0.18% of the input energy is consumed by the pumps. This internal power consumption by the system components is often referred to as 'parasitic power'. Further, about half of the gas turbine output is needed to pressurize the air flowing through the fuel cell and the turbine combustor to the 10 atm operating pressure.

The pressurized system shown in Fig. 3 is more efficient than the ambient pressure system shown in Fig. 2, despite the fact that more of the gross power is needed for gasifying the coal and deriving the fuel gas for the fuel cell than is needed for processing natural gas. The increased efficiency is obtained from thermally integrating the fuel cell with a bottoming cycle. This thermally integrated system can be optimized for efficiency or the net cost of electricity (COE). Figures 5 and 6 show how the system
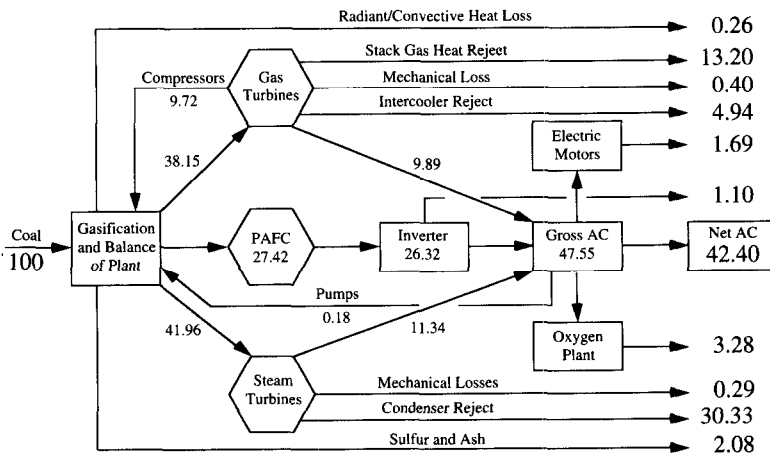


Fig. 4. Normalized energy flows, distribution, and losses in the phosphoric acid fuel cell system shown in Fig. 3.
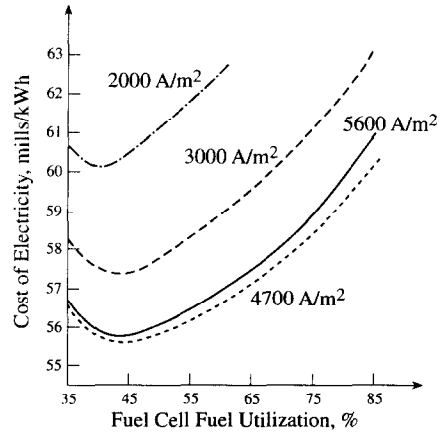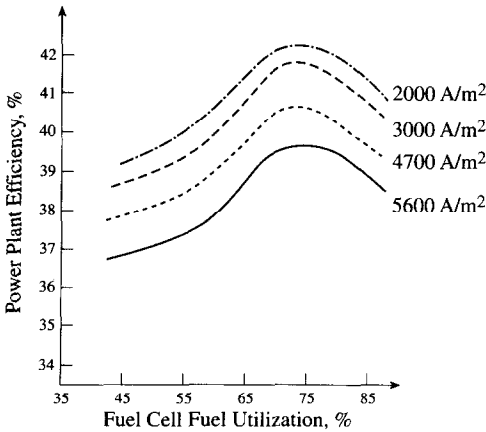
Fig. 5. Efficiency of the conceptual phosphoric acid fuel cell plant as a function of the electro-chemical fuel utilization and current density in the fuel cell stack.

Fig. 6. Cost of electricity for the conceptual phosphoric acid fuel cell plant as a function of the electrochemical fuel utilization for various current densities in the fuel cell stack.

efficiency and economics are affected by the electrochemical fuel utilization. The efficiency of the system peaks at about 75% fuel utilization, because the flame temperature in the turbine becomes too low if a higher fraction of the fuel is consumed in the fuel cell. The COE reaches a minimum at even lower fuel utilizations, because fuel cells are still considerably more expensive than turbines; using the fuel cells as a topping cycle for turbines is economically more attractive than generating all of the power in the fuel cells. Environmental considerations can, however, shift the balance of power generation between the fuel cells and the turbines.

It is also important to recognize the effect of current density on system efficiency and economics. Present-day PAFCs operate at current densities between 2000 and 3500 $A/m^2$. Figures 5 and 6 show that the higher the current density, the lower the system efficiency, because the higher current density lowers the operating cell voltage. Despite the lower efficiency, however, the system economics are better at higher current densities because of a concomitant decrease in active cell area and, hence, fuel cell costs.

*Chemical integration*

Converting a hydrocarbon fuel to hydrogen requires steam and heat, as discussed earlier regarding eqns. (7) and (8). The steam can be obtained from the water formed in the fuel cell as shown for the PAFC system. Because phosphoric acid and polymer electrolytes are proton conductors, the water in these cells is produced at the air electrodes; the steam, however, is needed on the fuel side. A condenser is therefore needed for the cathode exhaust to recover the water as a liquid, which must then be vaporized and reinjected into the fuel stream.

In MCFCs and SOFCs, the water is produced at the fuel electrodes, because the electrolytes conduct the oxygen from the cathode to the anode. The steam needed for the reforming reaction can, therefore, be obtained by simply recycling a portion of the depleted fuel into the fresh fuel stream. Further, the SOFCs and MCFCs operate at high enough temperatures to carry out the reforming reaction. Thus,

reforming can occur in the fuel cell itself and does not require a separate reforming reactor or a water condenser. This 'internal reforming' simplifies the system design and reduces the parasitic power requirements for cooling the stacks.

An example of such an internally reforming fuel cell system is the 25-kW SOFC prototype from Westinghouse Electric Corporation, see ref. 10, shown in Fig. 7. It makes use of a small pre-reformer inside the generator module to reform about 75% of the fuel; the rest of the fuel is reformed within the cell stack [11]. The pre-reformer is a small heat exchanger located underneath the stack that receives heat from the exhaust stream and steam from recirculated spent fuel. Preheating of air occurs in a recuperator, in the combustion zone above the cell stack. This system is quoted to have a gross efficiency of 45% and a net efficiency of 33% after accounting for the power consumed by blowers, pumps, controls, instrumentation, etc. [10]. In small, developmental systems such as this, parasitic power needs are relatively high. In addition, heat losses for such a small system are also relatively high due to the high external surface to volume ratio for the stack and the exhaust gas-to-inlet air recuperative heat exchanger. In their larger units, Westinghouse plans to more fully integrate reforming within the fuel cell stack to improve thermal management and reduce parasitic power requirements; they predict efficiencies of 45 to 50% for 100-kW or larger systems [11].

A second, highly integrated SOFC system designed at Argonne is shown in Fig. 8 [9]. It is pressurized and uses coal as fuel. The gasifier is an air-blown fluidized-bed gasifier with limestone injection [12], operating at a pressure of 30 atm. In this system, 90% of the sulfur is removed in the gasifier, and the rest is captured in a
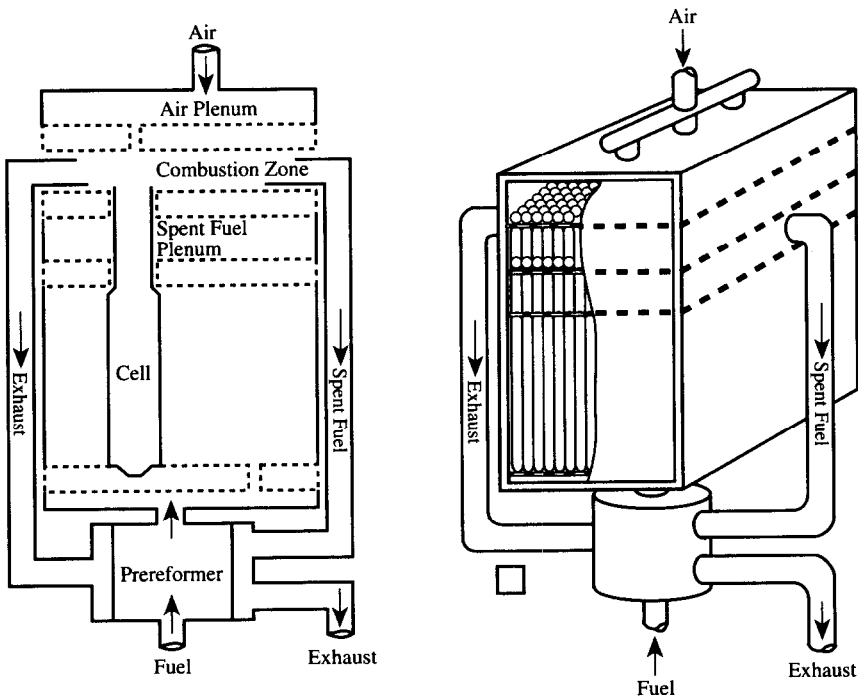


Fig. 7. The tubular Westinghouse solid oxide fuel cell and 25-kW generator operating on natural gas fuel.
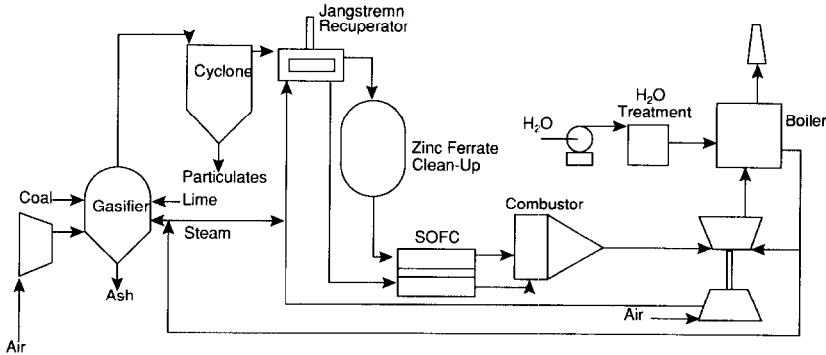
Fig. 8. Process flowsheet for an integrated coal-fueled solid oxide fuel cell plant design developed at Argonne.

hot-gas clean-up unit. A fuel utilization of 55% is used in the fuel cell stack; the rest of the fuel is burned to power a steam-injected gas turbine.

This conceptual coal-based SOFC system shown in Fig. 8 is much simpler than the conceptual PAFC system shown in Fig. 3, and was estimated to be less expensive. Simulations of the energy balance yielded net system efficiencies of 55% with about two-thirds of the power coming from the fuel cells and one-third from the turbine. The parasitic power requirements were 5% of the gross output.

## System economics

The examples given above show that gains in system efficiency are achievable but with added system complexity. Fuel cell system efficiencies depend on the operating voltage of the fuel cell, thermal integration with a bottoming cycle, and parasitic power requirements. The more integrated systems will usually require more components, and systems with many components are usually more expensive than simpler systems with fewer components. Clearly, optimizing the system for high efficiency will only be worthwhile where fuel costs are high and the costs of capital are low.

On the other hand, careful integration of the system's chemistry can limit the system's complexity and cost, and still yield exceptionally high efficiencies. Nevertheless, such system designs may require development of unconventional balance-of-plant components, such as the lime-injected gasifier, hot-gas desulfurizer, high-temperature blowers, and high-temperature heat exchangers and recuperators.

In this section, we discuss the relationship between system economics and efficiency, and the correlation between system cost and production volume.

### Cost versus efficiency

Figure 9 shows a schematic diagram of a 2-MW MCFC system for atmospheric pressure operation [13]. In the baseline mode of operating at a current density of 1600 $A/m^2$, this system was quoted as having an efficiency of 52.5% and was projected to cost US$ 1245/kW. For the assumed weighted cost of capital to a US utility of 3.7% (real) and a fuel cost of US$ 6.43/GJ (US$ 6.10 per million Btu), this system would generate electricity at a cost of US$ 0.0846/kWh.

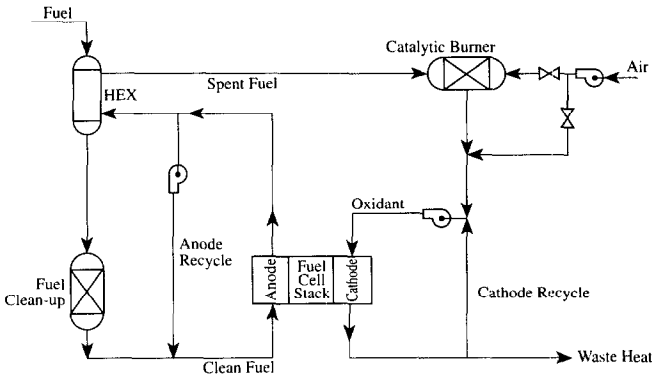Fig. 9. Schematic diagram for a 2-MW molten carbonate fuel cell power plant.

For a decrease in current density from 2000 to 1000 A/m$^2$, the system efficiency increases by 4.2%. However, the addition of more fuel cells to the system increases the plant cost by about US$ 300/kW, and the COE increases by about US$ 0.006/kWh. At an inflation-free cost of capital of 3.7% and a fuel cost of US$ 6.43/GJ, the higher efficiency is obviously not worth the additional capital investment. Of course, similar analyses with different parameters may yield very different results.

Incidentally, natural gas prices in the USA in 1993 were lower than they were in 1985. This further emphasizes the need to lower fuel cell system costs if such systems are to gain commercial acceptance.

*Production volume*

Viewed as a daydream by some, the use of fuel cells as potential replacements for internal combustion engines in transportation is being actively considered and promoted. The US Department of Energy initiated a program in 1987 to develop PAFC-powered buses; this was followed in 1990 with a program to develop PEFC-powered automobiles [14]. Shown in Fig. 10 is a system diagram for a methanol-fueled PEFC power source with a capacity of 60 kW [15]. Fuel is reformed and shifted analogously to the PAFC system, but an additional preferential oxidation step is needed to reduce the concentration of carbon monoxide to the low parts-per-million range. Unlike the 200-kW PAFC system, the PEFC system has to be pressurized and uses a turbocompressor to pressurize the air supplied to the cathode and to recover energy from the air leaving the cathode. This 60-kW PEFC system is clearly more complex than the 200-kW stationary PAFC power plant, yet to be viable in transportation, it would have to be manufactured for US$ 50–100/kW.

A cost estimate by a major automobile manufacturer based on learning-curve experience in mass-producing automotive components suggests that a PEFC system could be made for US$ 90/kW if produced at a rate of one million units per year. Implicit in such a projection are technology improvements relative to state-of-the-art PEFC systems. To put this projected cost in perspective, the relationship between the number of fuel cell systems manufactured and their cost is shown in Fig. 11. The first 56 PAFC units from ONSI were sold for US$ 2500/kW, although the actual costs were a bit higher; the cost of the next series of 700 units with more advanced technology is expected to decrease to about US$ 1500/kW [16]. Early SOFC systems are widely believed to have been sold for about US$ 100 000/kW, while prototype PEFC systems
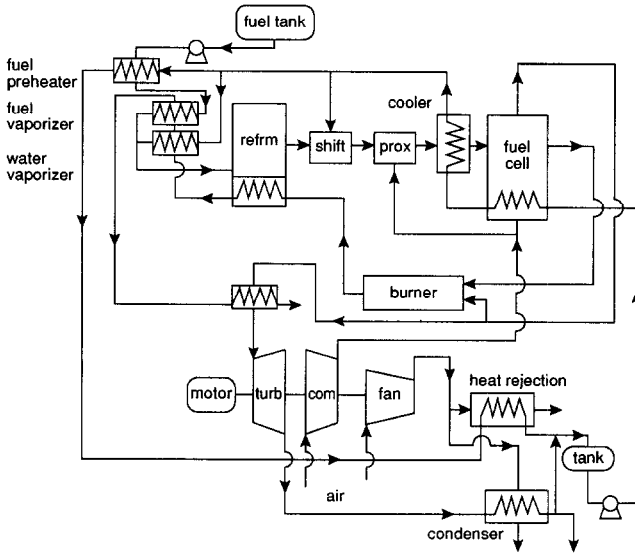
Fig. 10. System diagram of a methanol-fueled polymer electrolyte fuel cell power source for transportation application.
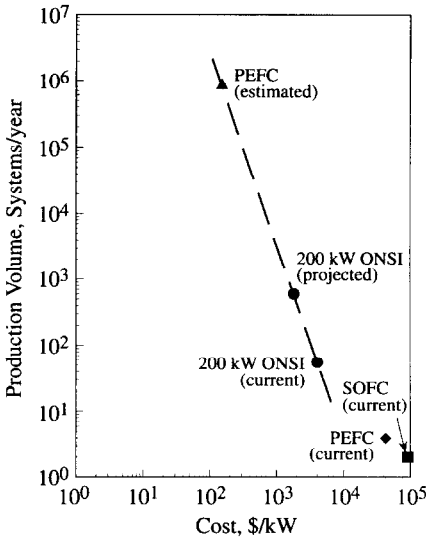


Fig. 11. The projected relationship between the number of fuel cell systems built per year and their manufacturing cost.

can be obtained for approximately US$ 50 000/kW. On the log-log scale used in Fig. 11, these data points correlate reasonably well with the US$ 90/kW cost for $10^6$ fuel cell systems built per year. The slope of the line agrees with the generic approximation that production costs decrease by one order of magnitude as the production volume increases by two orders of magnitude.

If these cost projections are borne out in the years to come, then fuel cell systems may indeed replace heat engines in many applications, and system complexity may well become a less critical issue than it is at present.

## Conclusions

In conclusion, system integration is the key to the successful introduction of fuel cells into the civilian economy. Systems can be optimized for efficiency or economics. High efficiencies are achieved by operating at low current densities, integration with a bottoming cycle, and minimizing parasitic power requirements. Very efficient systems are often more complex and hence more expensive than simpler, less efficient systems. At today's relatively low fuel costs, high efficiency is therefore not as important as low capital costs. To minimize capital costs, the fuel cell must be run at high current densities, and the balance-of-plant must be engineered to be as inexpensive as possible. However, once fuel cells are established and mass production methods can be applied, system complexity may become a less important issue, and efficiency can then be maximized.

## Acknowledgements

## References

1 A.J. Appleby and F.R. Foulkes, *Fuel Cell Handbook*, Van Nostrand Reinhold, New York, 1989.
2 K. Kinoshita, F.R. McLarnon and E.J. Cairns, *Fuel Cells — A Handbook, DOE/METC-88/6096*, 1988.
3 G.A. Eisman, *J. Power Sources, 29* (1990) 389.
4 H.C. Maru, L. Paetsch and A. Pigaud, *Molten Carbonate Fuel Cell Technology*, Proc. Vol. 84-13, The Electrochemical Society, Pennington, NJ, USA, 1984, p. 20.
5 H. Nafe, *Solid State Ionics, 13* (1984) 255.
6 K.B. Prater, *J. Power Sources, 37* (1992) 181.
7 D.T. Hooie, B.C. Harrington, M.J. Mayfield and E.L. Parsons, *Fuel Cells — Technology Status Rep., DOE/METC-92/0276*, 1992.
8 G.J. Sandelli, Demonstration of fuel cells to recover energy from landfill gas. Phase I. Final Rep. conceptual study, Rep. on US Environmental Protection Agency, *Contract 68-DI-0008.*
9 V. Minkov, E. Daniels, C. Dennis and M. Krumpelt, *Ext. Abstr., Fuel Cell Seminar, Tucson, AZ, USA, 1986*, Courtesy Associates, Washington, DC, USA, p. 255.
10 S. Takeuchi, A. Kusunok, H. Matsubara, Y. Kikuoka and J. Ohtsuki, *Proc. Third Int. Symp. Solid Oxide Fuel Cells, Honolulu, HI, USA, 1993*, The Electrochemical Society, Pennington, NJ, USA, 1993, p. 678.
11 C.A. Forbes, personal communication.

12 *Conf. Coal Gasification Systems and Synthetic Fuels for Power Generation,* Section 21, *EPRI-AP4757-SR,* Electric Power Research Institute, Palo Alto, CA, USA, 1985.

13 Parametric analysis of a 6500 Btu/kWh heat rate dispersed generator, *EPRI EM-4179,* 1985.

14 P.G. Patil, *J. Power Sources, 37* (1992) 171.

15 R.D. Sutton and N.E. Vanderborgh, *Proc. Annual Automotive Technology Development Contractors' Coordination Meet. 1992,* P-265, Society of Automotive Engineers, Warrendale, PA, USA, 1993, p. 493.

16 W. Lueckel, personal communication.